Taibah University

Journal of Taibah University Medical Sciences

www.sciencedirect.com

Original Article

Isolation, characterization, and docking studies of campesterol and β-sitosterol from *Strychnos innocua* (Delile) root bark

Ahmed Jibrin Uttu, PhD [a],[*], Muhammad Sani Sallau, PhD [b], Hamisu Ibrahim, PhD [b] and Ogunkemi Risikat Agbeke Iyun, PhD [b]

[a] *Department of Chemistry, Federal University Gashua, Yobe State, Nigeria*
[b] *Department of Chemistry, Ahmadu Bello University, Zaria, Nigeria*

المخلص

أهداف البحث: تشتهر فيتوستيرولس التي يتم الحصول عليها من النباتات الطبية بخصائصها المضادة للسكري والقلب والأوعية الدموية والسرطان والمضادة للميكروبات. ينمو الإسطركن الشوكي (عضو في عائلة اللوغانيات) في العديد من الدول الأفريقية وغالبا ما يستخدم للأغراض الطبية.

طرق البحث: أدى الفصل الكروماتوجرافي لمستخلص أسيتات الإيثيل من الإسطركن الشوكي (لحاء الجذر) إلى عزل كامبيسترول (1) وبيتا سيتوستيرول (2).

النتائج: تم تأكيد هياكلها عن طريق قياس الطيف الكتلي والرنين المغناطيسي النووي وبيانات الأدب. هذا هو تقرير جديد عن كامبيسترولوبيتاسيتوستيرول من النبات. كشفت دراسات الالتحام أن ارتباطات الارتباط 1 مع مواقع الربطللمكورات العنقودية الذهبية بيروفاتالكربوكسيلاز ومنظمعامل الفوعة الزائفة الزنجارية كانت -7.8 و -7.9 كيلو كالوري /مول،على التوالي. علاوة علىذلك،يحتوي 2 على ارتباطات ملزمة تبلغ -7.6 و -7.7 كيلو كالوري / مول مع مواقع الربطل المكورات العنقودية الذهبيةوالزائفةالزنجارية،علىالتوالي،بينما يحتوي سيبروفلوكساسين (دواء قياسي) على ارتباطات ملزمة -6.6 و -8.7 كيلو كالوري / مول.

الاستنتاجات: أشارت هذه الدراسة إلى أن لحاء جذر الإسطركن الشوكي يحتوي على وجود غني من كامبيسترول وبيتا سيتوستيرول، وأن تحقيقات الالتحام الجزيئي في سيليكو أظهرت أن المركبات تتفاعل بشكل جيد مع مواقع ارتباط الزائفة الزنجارية والمكورات العنقودية الذهبية.

Abstract

Objectives: Phytosterols obtained from medicinal plants are well known for their anti-diabetic, anti-cardiovascular, anti-cancer, and anti-microbial properties. *Strychnos innocua* (a member of the Loganiaceae family) grows in several African nations and is frequently used for medicinal purposes.

Methods: The chromatographic separation of *S. innocua* (root bark) ethyl acetate extract resulted in the isolation of campesterol (**1**) and β-sitosterol (**2**).

Results: The structures of **1** and **2** were confirmed by mass spectrometry, nuclear magnetic resonance (1D and 2D NMR), and literature data. This is a novel report of campesterol and β-sitosterol from *S. innocua*. Docking studies revealed that the binding affinities of **1** with the binding sites of *Staphylococcus aureus* pyruvate carboxylase (PDB: 3HO8) and *Pseudomonas aeruginosa* virulence factor regulator (PDB: 2OZ6) were −7.8 and −7.9 kcal/mol, respectively. Furthermore, **2** had binding affinities of −7.6 and −7.7 kcal/mol with binding sites of *S. aureus* and *P. aeruginosa*, respectively, whereas ciprofloxacin (a standard drug) had binding affinities of −6.6 and −8.7 kcal/mol.

Conclusion: This study indicated that *S. innocua* root bark is rich in campesterol and β-sitosterol. *In silico* molecular docking demonstrated that the compounds interact well with the binding sites of *S. aureus* and *P. aeruginosa*.

* Corresponding address: Department of Chemistry, Federal University Gashua, Yobe State, Nigeria.
E-mails: jibuttu@yahoo.com (A.J. Uttu), sskaraye@yahoo.com (M.S. Sallau), hibrahimbk@yahoo.com (H. Ibrahim), kemiruthiyun@gmail.com (O.R.A. Iyun)

ELSEVIER | **Production and hosting by Elsevier**

Introduction

Compounds derived from plants have enormous potential for the development of new drugs.[1] The various parts of plants (leaves, stems, roots, fruit, and flowers) are used in multiple applications, including medicinal purposes.[2]

In medicinal plants, the phytochemicals and secondary metabolites, such as phytosterols, contain active medicinal components with therapeutic potential.[3,4] Campesterol is a naturally occurring plant sterol that has been associated with cholesterol lowering and cancer prevention.[5] *Plumbago zaylanica* contains β-sitosterol, which has antibacterial, antimalarial, antifertility, anti-inflammatory, blood coagulation, wound healing, and anticancer properties.[6]

Several approaches, such as in vitro, in vivo, and in silico methods, have been used to investigate the antimicrobial activity of natural plant constituents. Docking is one technique that has seen widespread use in the development of antimicrobial medicines.[7,8]

Strychnos innocua (Figure 1) is a plant of the Loganiaceae family with a straight stem and a height up to 18 m. It has a trunk diameter ranging from 7 to 40 cm, and many branches. Its leaves are normally simple, with a rounded base in rare instances. *S. innocua* can be found in Cameroon, Malawi, and Nigeria. The root bark of the plant has been reported to cure gonorrhea, and a fresh infusion of the plant's root is used to treat snake bites.[9,10] The plant can be harvested in Kaduna State, Nigeria.

The chemical compositions and antimicrobial activities of *S. innocua* root bark extracts have been investigated.[11–15] However, research on the isolation of phytosterols from *S. innocua* root bark is lacking. Herein, the phytosterols campesterol (**1**) (Figure 2) and β-sitosterol (**2**) (Figure 3) were isolated from the root bark of *S. innocua*, characterized, and docked to assess their antibacterial activity. This is a novel report of phytosterol compounds from the plant root bark.

Materials and Methods

Plant collection

S. innocua was obtained in the wild in Kaduna State, Nigeria. Mr. Namadi Sunusi identified and authenticated the specimen at the Department of Biological Sciences at ABU, Zaria, where V/N-01884 is the herbarium voucher number.

Extraction

The root bark of *S. innocua* was dried in the shade, then crushed to a fine powder. According to a prior report,[11] the powder (i.e., crushed sample, 2 kg) was subjected to extraction with the maceration method with solvents *n*-hexane (HEX), ethyl acetate (EA), and methanol, with increasing polarity.

General experimental procedure

GC−MS analysis of the isolated compounds was performed on a GC 7890B, MSD 5977A, Agilent Tech instrument. The carrier gas used was helium at a flow rate of 1 mL/min. The sample supernatant (1 μL) was injected into the GC while the temperature of the GC oven was set to rise from 80 °C to 150 °C at a rate of 12 °C/min, then to 270 °C at a rate of 9 °C/min, followed by a 5-min isothermal step at 325 °C. The ion source temperature was set at 230 °C, and the ionization voltage was set to 70 eV. The NMR (1D and 2D) spectra were obtained on a Varian−Vnmrs 400 MHz spectrometer with chloroform ($CdCl_3$). Chemical shifts (δ) are reported in ppm.

The chemicals and reagents used in the investigation were of analytical grade.

Isolation and purification

With several solvent systems, thin layer chromatography (TLC) of ethyl acetate extract revealed many spots. The extract (30 g) was mixed with 60−120 mesh silica gel and dried. After parking (with silica gel and HEX), the dried extract was placed in a column (size, 5 × 60 cm) and eluted with a suitable solvent (HEX:EA) under gradually increasing polarity (HEX 100%, 9:1, 8:2, 7:3, 6:4, 1:1, 4:6, 3:7, 2:8, 1:9, and 100% EA) at a flow rate of 1 drop/sec, thereby yielding 261 collections of 50 mL. To monitor these collections, we used TLC plates pre-coated with spraying reagent ($CH_3OH:CH_3COOH:H_2SO_4:CH_3OC_6H_4CHO$ at a ratio of 85:10:5:0.l mL), thus generating 24 fractions (F1−F24). Fractions 8 and 9 were mixed and separated with column chromatography with increasing concentrations of HEX:EA (HEX 100%, HEX:EA, 9:1) to obtain 60 collections of 5 mL each. A pre-coated TLC plate was also used to monitor the collections, thus yielding eight subfractions (FF1−FF8). The FF4 and FF5 subfractions were further combined and separated on a column before being eluted with HEX:EA (9.1), thus yielding three smaller fractions (SF1, SF2, and SF3). On TLC, SF2 revealed one spot representing compound **1** ($R_f = 0.41$), thus yielding 46 mg. FF2 and FF3 were combined and eluted with HEX:EA (9:1), and four smaller fractions (SF1, SF2, SF3, and SF4) were obtained. On TLC, SF3 revealed one spot, which was used to obtain compound **2** ($R_f = 0.18$), with a yield of 37 mg.

Molecular docking study

Compounds **1** and **2**, as well as ciprofloxacin (standard drug), were docked in silico with target receptors (PDB: 3HO8, and 2OZ6) obtained from the Protein Data Bank (www.rcsb.org). ChemDraw professional 16.0 was used to design its two-dimensional (2D) structure, which was subsequently optimized in three dimensions with Spartan 20v.1.1/2020. The target receptors were created in three dimensions with Discovery Studio Visualizer, saved in PDB file

format, and then uploaded to the Pyrx program for docking. To investigate protein—ligand interactions, the docking output was shown in Discovery Studio together with the binding energy.[16,17]

Results and discussion

Compound **1** (46 mg), in the form of a white powder, had a melting point of 162 °C. The mass spectrum (Figure 4) of **1** at retention time (R_T = 10.880 min) showed peaks at an m/z of 400, with molecular ion and fragment ion m/z values of 367, 316, 289, 255, 213, 173, 145, 109, 81, and 43, thus suggesting a molecular formula of $C_{28}H_{48}O$. The NMR spectra data (Table 1) of **1** was highly similar to that of campesterol in the literature, with ^{1}H NMR (Figure 5) displaying δ_H for one olefinic methine proton (δ_H 5.51 H-6), one hydroxyl proton (δ_H 4.53 OH), six methyl protons (δ_H 0.83 H-18, 0.67 H-19, 0.81 H-21, 0.77 C-26, 0.80 H-27, and 0.66 C-28), ten methylene protons (δ_H 1.99 H-1, 1.82 H-2, 1.60 H-4, 1.13 H-7, 1.12 H-11, 1.20 H-12, 2.12 H-15, 1.92 H-16, 2.20 H-22, and 1.08 H-23), and eight methine protons (δ_H 3.53 H-3, 1.80 H-8, 0.98 H-9, 1.46 H-14, 1.80 H-17, 2.27 H-20, 0.90 H-24, and 1.27 H-25). The ^{13}C NMR (Figure 6) and DEPT revealed 28 carbon signals for six methyl carbons (δ_C 15.58 C-18, 12.19 C-19, 14.35 C-21, 21.28 C-26, 20.01 C-27, and 15.64 C-28), ten methylene carbons (δ_C 37.44 C-1, 31.85 C-2, 42.49 C-4, 32.12 C-7, 23.25 C-11, 39.97 C-12, 24.51 C-15, 26.22 C-16, 34.31 C-22, and 34.13 C-23), eight methine carbons (δ_C 72.03 C-3, 32.09 C-8, 51.44 C-9, 56.96 C-14, 56.23 C-17, 36.35 C-20, 39.25 C-24, and 33.90 C-25), three quaternary carbons (δ_C 145.43 C-5, 36.71 C-10, and 46.01 C-13), and one olefinic methine carbon (δ_C 121.94 C-6) (see Table 2).

Compound **2** (37 mg), in the form of a clear crystal, had a melting point of 147 °C. The mass spectrum (Figure 7) of **2** at retention time (R_T = 27.486 min) indicated fragment ion peaks at an m/z of 396, representing a H_2O loss from the molecular ion peak (m/z 414). Other fragmentation ions
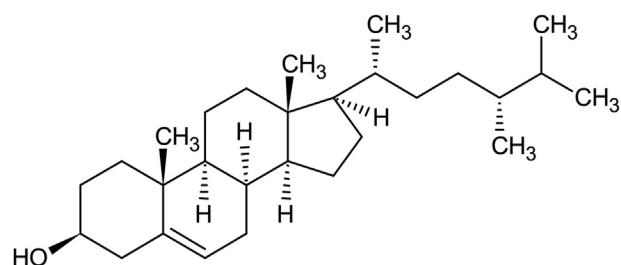

Figure 2: Structure of campesterol (**1**).

included m/z of 381, 342, 303, 255, 213, 173, 145, 109, 81, and 43, thereby suggesting a molecular formula of $C_{29}H_{50}O$. The NMR spectra data (Table 1) of **2** were highly similar to those in the literature for β-sitosterol, with ^{1}H NMR (Figure 8) displaying δ_H for six methyl protons (δ_H 0.87 H-18, 0.78 C-19, 0.97 H-21, 0.82 H-26, 0.85 H-27, and 0.88 H-29), eleven methylene protons (δ_H 1.72 H-1, 1.93 C-2, 2.32 H-4, 1.95 H-7, 1.19 H-11, 1.22 H-12, 1.53 H-15, 1.20 H-16, 1.43 H-22, 1.22 H-23, and 1.39 H-28), nine methine protons (δ_H 3.57 H-3, 5.46 H-6, 2.19 H-8, 1.10 H-9, 1.15 H-14, 1.21 H-17, 1.51 H-20, 1.14 C-24, and 1.57 H-25), and one hydroxyl proton (δ_H 4.82 OH). The ^{13}C NMR (Figure 9) and DEPT displayed 29 carbon signals for six methyl carbons (δ_C 14.31 C-18, 19.52 C-19, 20.70 C-21, 22.86 C-26, 22.81 C-27, and 14.35 C-29), eleven methylene carbons (δ_C 38.89 C-1, 30.27 C-2, 41.25 C-4, 32.14 C-7, 22.91 C-11, 40.09 C-12, 28.95 C-15, 28.88 C-16, 33.20 C-22, 28.98 C-23, and 24.85 C-28), eight methine carbons (δ_C 72.06 C-3, 31.88 C-8, 51.46 C-9, 56.52 C-14, 55.00 C-17, 33.77 C-20, 45.02 C-24, and 29.91 C-25), three quaternary carbons (δ_C 143.71 C-5, 37.34 C-10, and 43.51 C-13), and one olefinic methine carbon (δ_C 122.21 C-6).

The ethyl acetate extract demonstrated the presence of steroids in the phytochemical investigation, and further displayed potent antibacterial action against *S. aureus, P. aeruginosa,* and *B. subtilis.*[13] Campesterol and β-sitosterol were isolated from the extract after chromatographic separation, and their structures (Figures 2 and 3) were identified with spectroscopic investigations and comparison with data from the literature.[18–23] These compounds are present in a variety of plant species; their biological activities have been
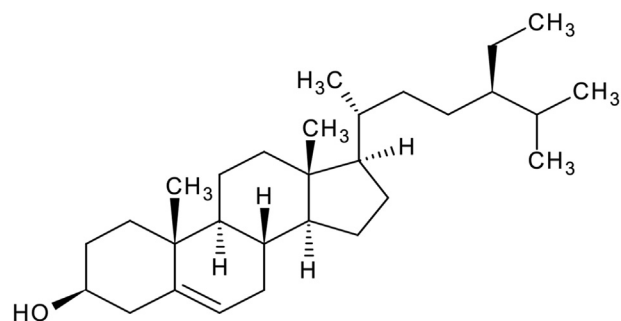

Figure 1: *Strychnos innocua* branches fruit, and leaves.

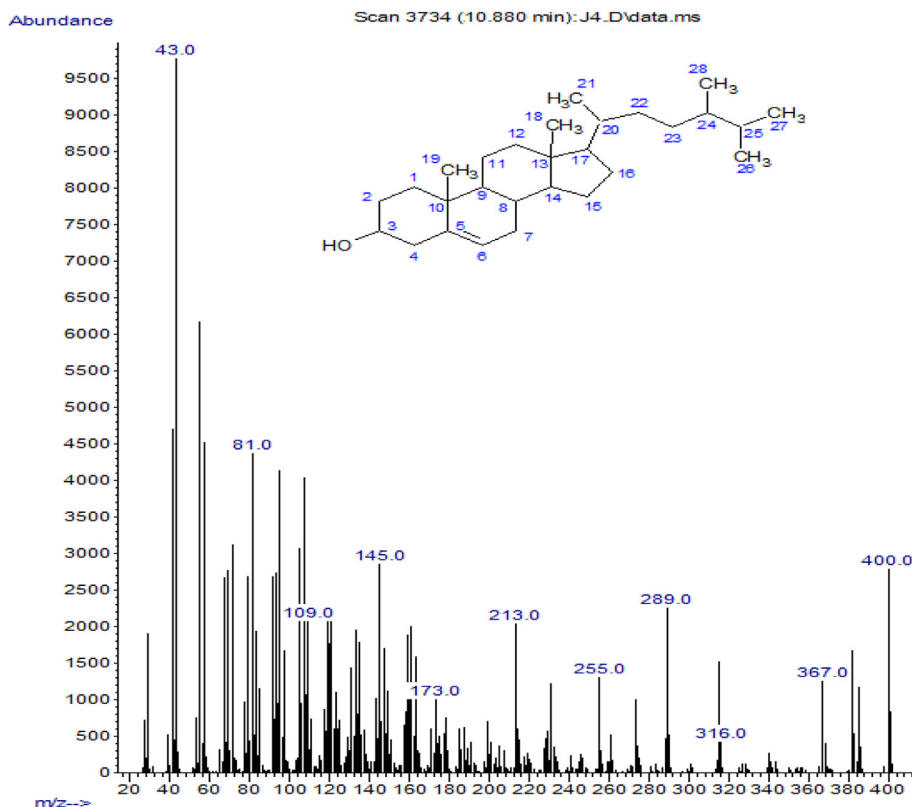**Figure 3:** Structure of β-sitosterol (**2**).

Figure 4: Mass spectrum of campesterol (**1**).

Table 1: NMR (400 MHz, CDCl₃) data for campesterol (1).

Position	Campesterol			Literature data[18,19]		
	^{1}H (ppm)	^{13}C (ppm)	DEPT	^{1}H (ppm)	^{13}C (ppm)	DEPT
C-1	1.99 (m, 2H)	37.44	CH$_2$	1.55 (m, 2H)	37.30	CH$_2$
C-2	1.82 (m, 2H)	31.85	CH$_2$	1.52 (m, 2H)	28.90	CH$_2$
C-3	3.53 (m, 1H)	72.03	CH	3.40 (m, 1H)	71.90	CH
C-4	1.60 (m, 2H)	42.49	CH$_2$	1.40 (m, 2H)	42.30	CH$_2$
C-5		145.43	C		142.40	C
C-6	5.51 (m, 1H)	121.94	CH	5.31 (m, 1H)	121.90	CH
C-7	1.13 (m, 2H)	32.12	CH$_2$	1.33 (m, 2H)	31.80	CH$_2$
C-8	1.80 (m, 1H)	32.09	CH	1.73 (m, 1H)	31.00	CH
C-9	0.98 (m, 1H)	51.44	CH		51.20	CH
C-10		36.71	C		36.50	C
C-11	1.12 (m, 2H)	23.25	CH$_2$	1.13 (m, 2H)	21.10	CH$_2$
C-12	1.20 (m, 2H)	39.97	CH$_2$	1.21 (m, 2H)	39.80	CH$_2$
C-13		46.01	C		43.10	C
C-14	1.46 (m, 1H)	56.96	CH	1.83 (m, 1H)	56.90	CH
C-15	2.12 (m, 2H)	24.51	CH$_2$		21.80	CH$_2$
C-16	1.92 (m, 1H)	26.22	CH$_2$	1.92 (m, 1H)	25.00	CH$_2$
C-17	1.80 (m, 1H)	56.23	CH	1.73 (m, 1H)	56.10	CH
C-18	0.83 (s, 3H)	15.58	CH$_3$	1.10 (s, 3H)	19.80	CH$_3$
C-19	0.67 (s, 3H)	12.19	CH$_3$	0.73 (s, 3H)	12.20	CH$_3$
C-20	2.27 (m, 2H)	36.35	CH	2.17 (m, 1H)	32.50	CH
C-21	0.81 (d, 3H)	14.35	CH$_3$	0.81 (d, 3H)	19.10	CH$_3$
C-22	2.20 (m, 2H)	34.31	CH$_2$		34.50	CH$_2$
C-23	1.08 (m, 2H)	34.13	CH$_2$	1.20 (m, 2H)	30.30	CH$_2$

(*continued on next page*)

Table 1 (*continued*)

| Position | Campesterol | | | Literature data[18,19] | | |
	^{1}H (ppm)	^{13}C (ppm)	DEPT	^{1}H (ppm)	^{13}C (ppm)	DEPT
C-24	0.90 (m, 1H)	39.25	CH	1.08 (m, 2H)	42.40	CH
C-25	1.27 (m, 1H)	33.90	CH	1.77 (m, 1H)	36.10	CH
C-26	0.77 (d, 3H)	21.28	CH$_3$	0.83 (d, 3H)	21.20	CH$_3$
C-27	0.80 (d, 3H)	20.01	CH$_3$	0.79 (d, 3H)	19.10	CH$_3$
C-28	0.66 (d, 3H)	15.64	CH$_3$	0.70 (d, 3H)	15.39	CH$_3$
OH	4.53 (s, 1H)					

thoroughly investigated, and their pharmaceutical effects have been established. The antifungal activity of campesterol and β-sitosterol obtained from *Dendrocalamus asper* against some fungal pathogens has been determined, and they have been found to have exceptional antifungal properties.[24] These compounds have also been shown to have anti-inflammatory, antibacterial, and anti-tumor effects.[25] In general, approximately 250 phytosterols are found in plants,
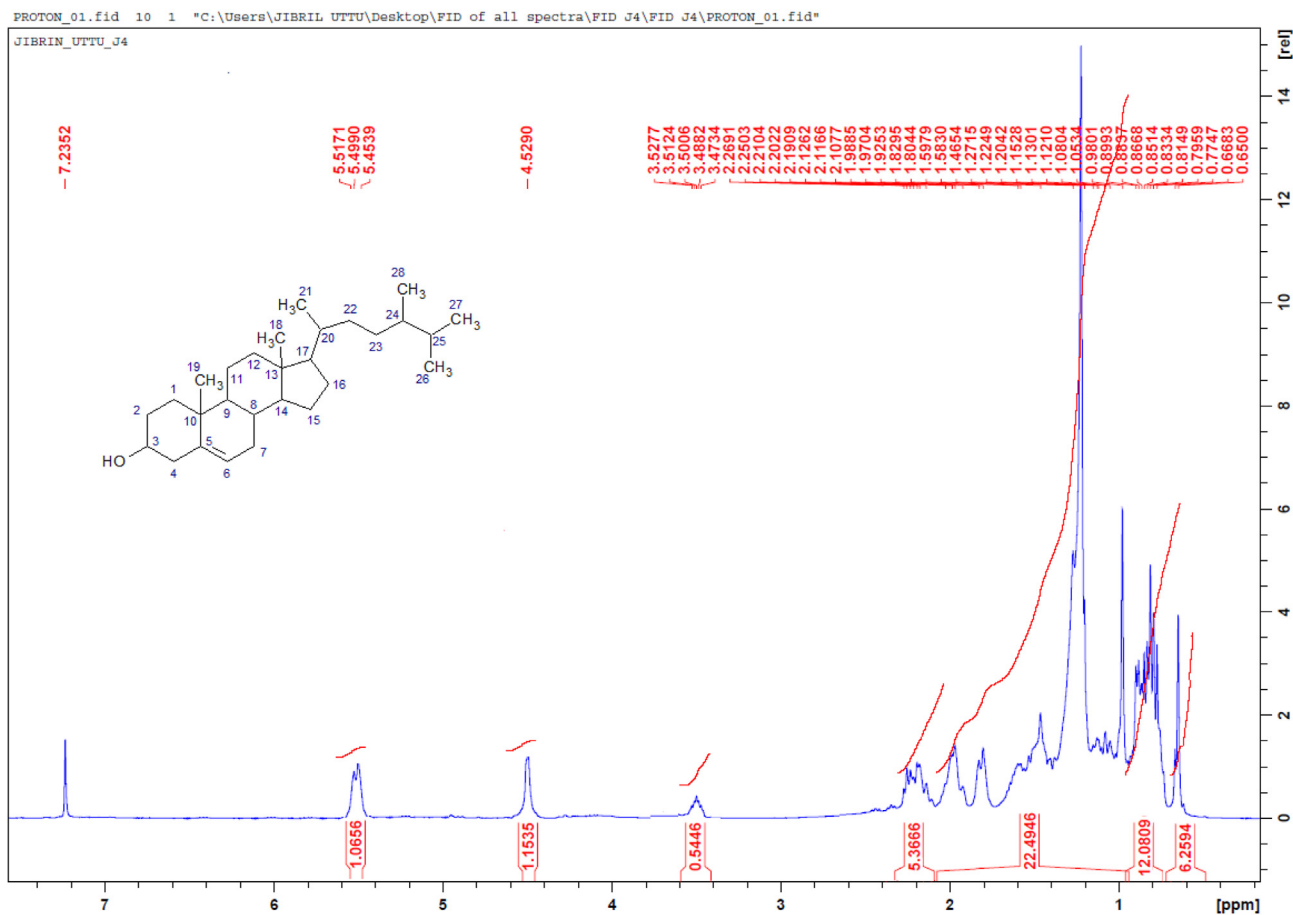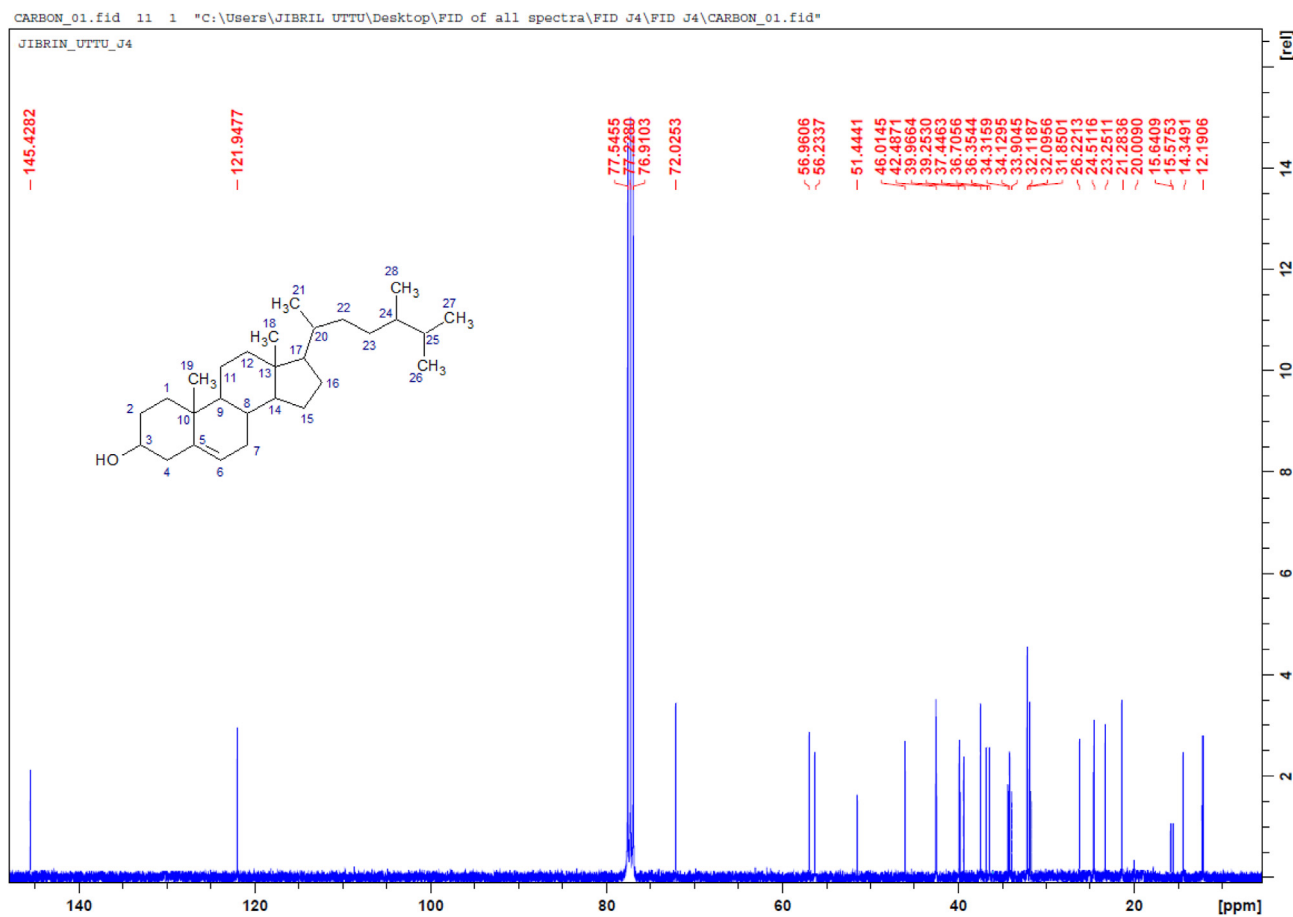

Figure 5: ^{1}H NMR spectrum of campesterol (**1**).
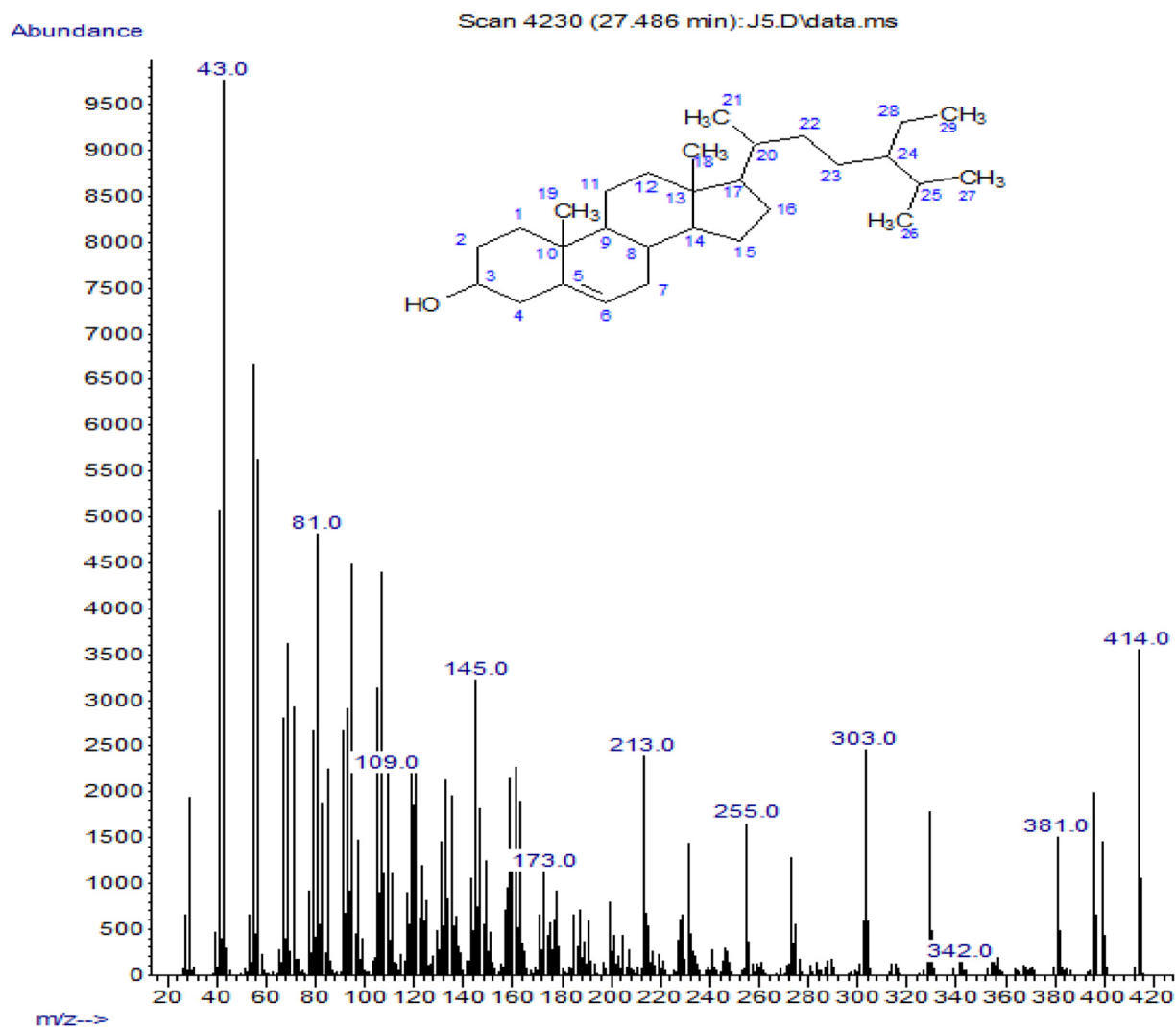
Figure 6: ^{13}C NMR spectrum of campesterol (**1**).

Table 2: NMR (400 MHz, CDCl₃) data for β-sitosterol (2).

Position	β-sitosterol			Literature data[20,21]		
	^1H (ppm)	^{13}C (ppm)	DEPT	^1H (ppm)	^{13}C (ppm)	DEPT
C-1	1.72 (m, 2H)	38.89	CH_2	1.85 (m, 2H)	37.39	CH_2
C-2	1.93 (m, 2H)	30.27	CH_2	1.95 (m, 2H)	31.76	CH_2
C-3	3.57 (m, 1H)	72.06	CH	3.55 (m, 1H)	71.95	CH
C-4	2.32 (m, 2H)	41.25	CH_2	2.38 (m, 2H)	42.39	CH_2
C-5		143.71	C		140.85	C
C-6	5.46 (m, 1H)	122.21	CH	5.37 (m, 1H)	121.85	CH_2
C-7	1.95 (m, 2H)	32.14	CH_2	1.99 (m, 2H)	32.06	CH_2
C-8	2.19 (m, 1H)	31.88	CH	2.00 (m, 1H)	31.93	CH
C-9	1.10 (m, 1H)	51.46	CH	0.94 (m, 1H)	50.28	CH
C-10		37.34	C		36.64	C
C-11	1.19 (m, 2H)	22.91	CH_2	1.02 (m, 2H)	21.22	CH_2
C-12	1.22 (m, 2H)	40.09	CH_2	1.16 (m, 2H)	39.92	CH_2
C-13		43.51	C		42.46	C
C-14	1.15 (m, 1H)	56.52	CH	1.00 (m, 1H)	56.90	CH
C-15	1.53 (m, 2H)	28.95	CH_2	1.58 (m, 2H)	28.39	CH_2
C-16	1.20 (m, 2H)	28.88	CH_2	1.09 (m, 2H)	28.35	CH_2
C-17	1.21 (m, 1H)	55.00	CH	1.12 (m, 1H)	56.18	CH
C-18	0.87 (s, 3H)	14.31	CH_3	0.85 (s, 3H)	12.12	CH_3
C-19	0.78 (s, 3H)	19.52	CH_3	0.82 (s, 3H)	19.40	CH_3
C-20	1.51 (m, 1H)	33.77	CH	1.35 (m, 1H)	36.29	CH
C-21	0.97 (d, 3H)	20.70	CH_3	0.95 (d, 3H)	18.92	CH_3

(*continued on next page*)

Table 2 (*continued*)

| Position | β-sitosterol | | | Literature data[20,21] | | |
	^{1}H (ppm)	^{13}C (ppm)	DEPT	^{1}H (ppm)	^{13}C (ppm)	DEPT
C-22	1.43 (m, 2H)	33.20	CH$_2$	1.33 (m, 2H)	34.07	CH$_2$
C-23	1.22 (m, 2H)	28.98	CH$_2$	1.16 (m, 2H)	26.14	CH$_2$
C-24	1.14 (m, 1H)	45.02	CH	0.94 (m, 1H)	45.99	CH
C-25	1.57 (m, 1H)	29.91	CH	1.66 (m, 1H)	28.91	CH
C-26	0.82 (d, 3H)	22.86	CH$_3$	0.83 (d, 3H)	21.38	CH$_3$
C-27	0.85 (d, 3H)	22.81	CH$_3$	0.84 (d, 3H)	19.18	CH$_3$
C-28	1.39 (m, 2H)	24.85	CH$_2$	1.25 (m, 2H)	23.20	CH$_2$
C-29	0.88 (m, 3H)	14.35	CH$_3$	0.85 (m, 3H)	12.19	CH$_3$
OH	4.82 (s, 1H)					

Figure 7: Mass spectrum of β-sitosterol (**2**).

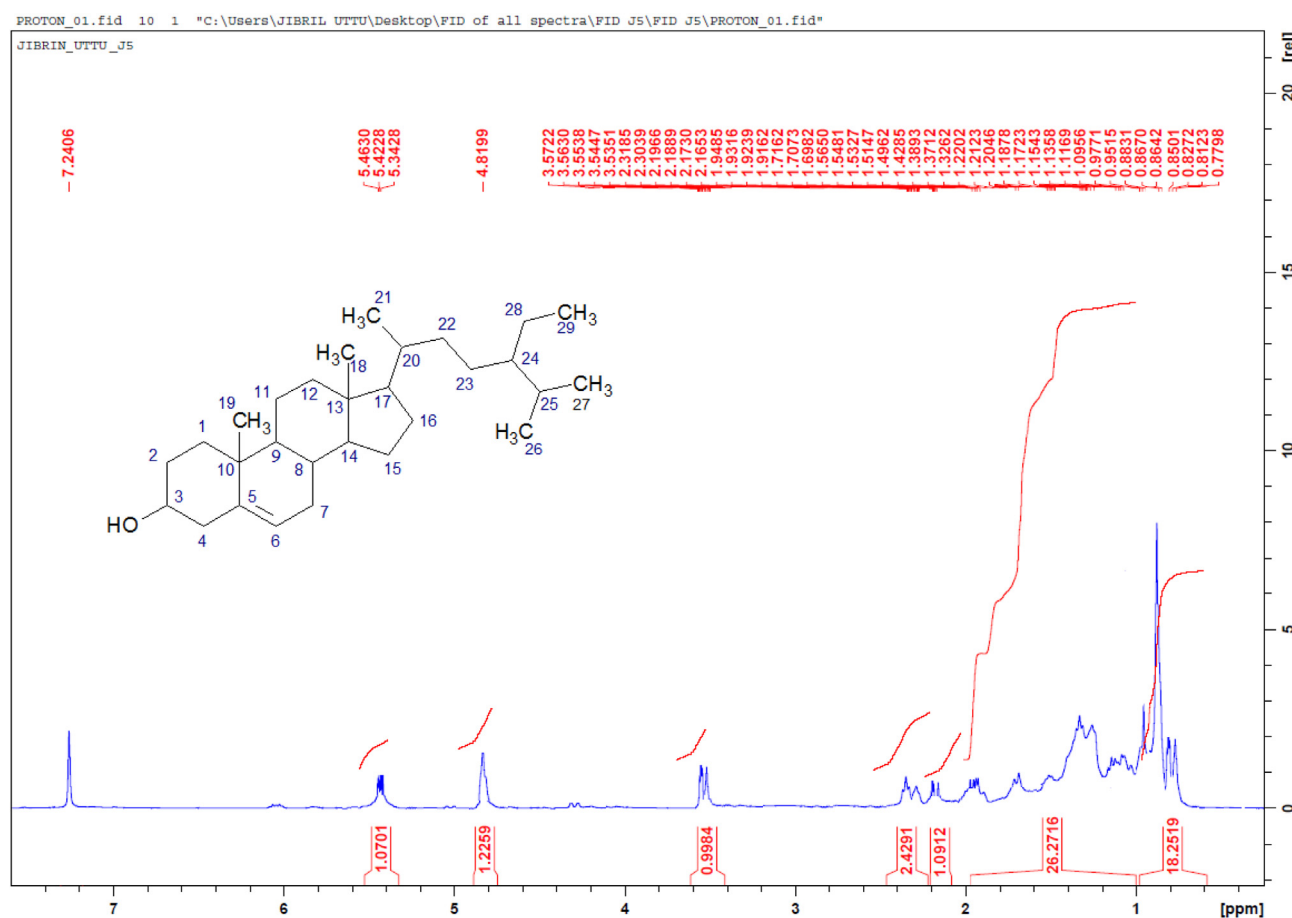**Figure 8:** ^{1}H NMR spectrum of β-sitosterol (**2**).

including sitosterol, stigmasterol, campesterol, brassicasterol, ergosterol, and β-sitosterol. They are related to cholesterol and, according to their structural components, have been identified in plant biological membranes.[26]

The interactions of the compounds with the target receptors (PDB: 3HO8 and 2OZ6) were studied with molecular docking and compared with those of ciprofloxacin (standard drug). Compounds **1** and **2** exhibited considerably greater binding energy (Table 3) toward *S. aureus* pyruvate carboxylase, 3HO8 (receptor) than ciprofloxacin. Campesterol had a greater binding energy (−7.8 kcal/mol) than β-sitosterol (−7.6 kcal/mol); their interactions with the receptor are shown in Figures 10 and 11, respectively. The binding energy of ciprofloxacin was −6.6 kcal/mol, and its interaction with the receptor is represented in Figure 12. These figures also indicate that the target residues involved in interactions with the docked compounds included PHE, PRO, LYS, VAL, PHE, TYR, and GLY, thus emphasizing the relevance of these residues in *S. aureus*

suppression. *S. aureus* has long been associated with soft tissue infections and skin conditions, such as food poisoning, abscesses, respiratory infections, furuncles, pneumonia, cellulitis, and joint infections.[27] Campesterol isolated from *Fiscus religiosa* shows substantial interactions with binding sites in the crystal structure of the Kelch−Neh2 complex (PDB: 2FLU), thus suggesting that it is a viable competitive agent to counteract Keapl and hence may be used in cancer chemoprevention (28).

Furthermore, compounds **1** and **2** had considerably lower binding energy (Table 4) than ciprofloxacin toward the *P. aeruginosa* virulence factor regulator 2OZ6 (receptor). Campesterol had a higher binding energy (−7.9 kcal/mol) than β-sitosterol (−7.7 kcal/mol), and their interactions with the receptor are shown in Figures 13 and 14, respectively. Ciprofloxacin's binding energy was −8.7 kcal/mol, and Figure 15 displays its interaction with the receptor. The target residues (LEU, ILE, and ARG) were involved in interactions with **1**, **2**,
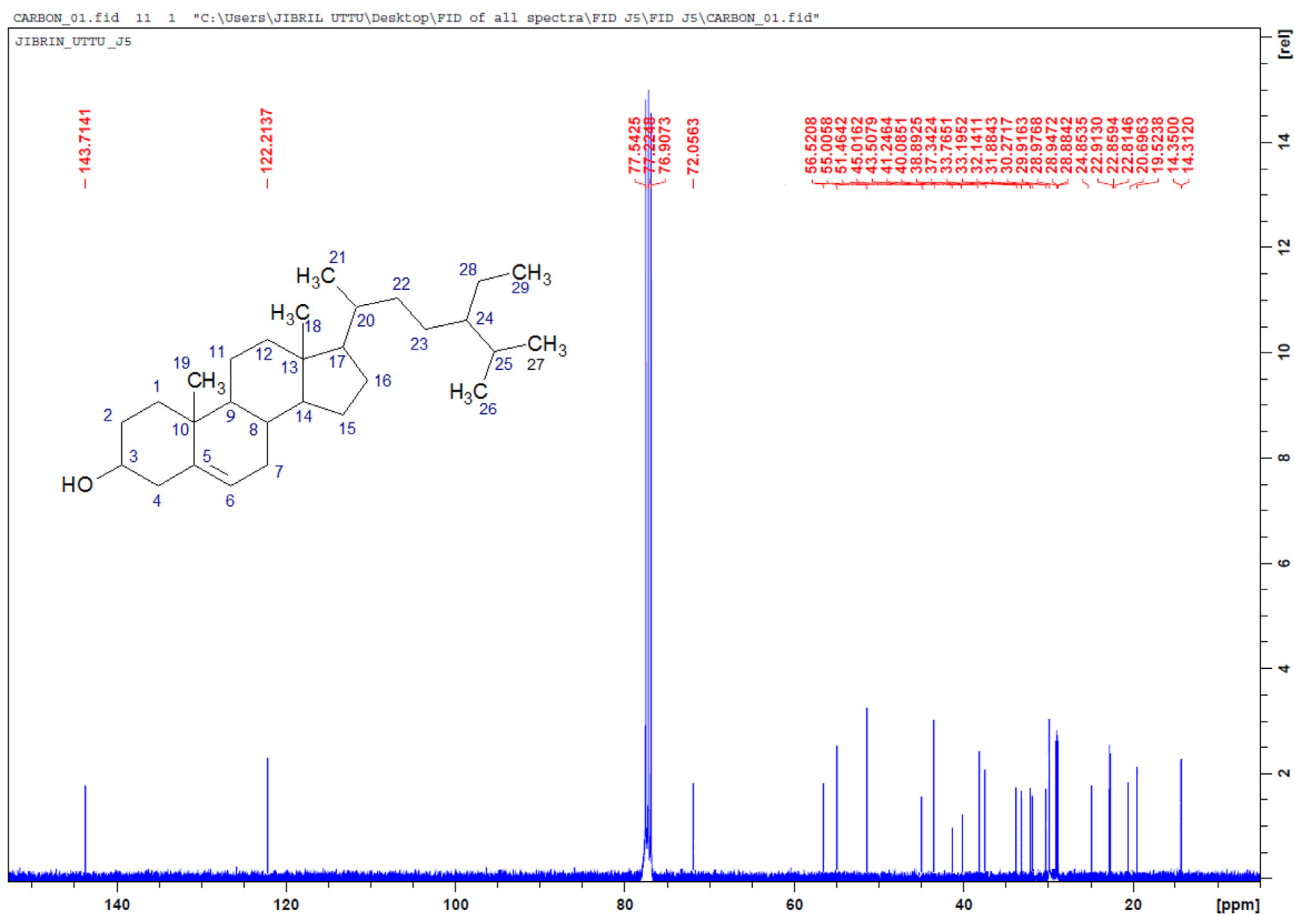
Figure 9: ^{13}C NMR spectrum of β-sitosterol (**2**).

Table 3: Binding energy of isolated compounds/ciprofloxacin with receptor (PDB: 3HO8).

Ligands	Binding score (kcal/mol)	Protein interaction	Types of interaction	Bond distance Å
Campesterol	−7.8	PHE516	Alkyl	4.74
		PRO410	Alkyl	5.03
		PRO410	Alkyl	5.46
		PRO410	Alkyl	5.16
		LYS518	Alkyl	4.92
		LYS518	Alkyl	5.46
		LYS518	Alkyl	4.23
		VAL404	Alkyl	4.37
		PHE516	Pi-alkyl	5.42
		TYR400	Pi-alkyl	5.37
		TRY400	Pi-alkyl	5.27
		GLY408	Carbon hydrogen bond	2.81
β-sitosterol	−7.6	PRO410	Alkyl	4.97
		PRO410	Alkyl	4.00
		PRO410	Alkyl	4.70
		LEU926	Alkyl	5.03
		LYS518	Alkyl	5.25
		LYS518	Alkyl	4.77
		LYS518	Alkyl	4.14
		VAL404	Alkyl	4.79
		PHE516	Pi-alkyl	4.81

Table 3 (*continued*)

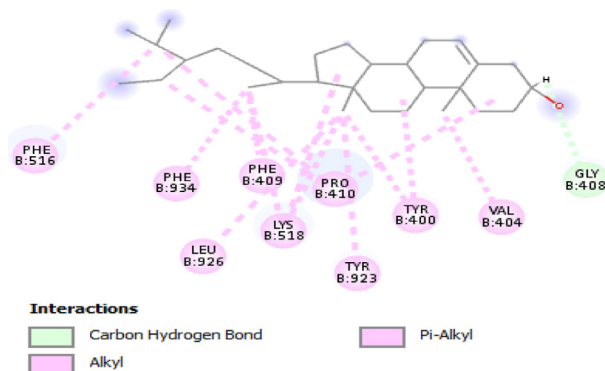| Ligands	Binding score (kcal/mol)	Protein interaction	Types of interaction	Bond distance Å
		PHE409	Pi-alkyl	4.68
		PHE934	Pi-alkyl	5.13
		TYR400	Pi-alkyl	5.06
		TYR400	Pi-alkyl	4.61
		TRY923	Pi-alkyl	4.77
		GLY408	Carbon hydrogen bond	2.99
Ciprofloxacin	−6.6	PRO410	Pi-sigma	3.70
		PHE934	Pi-alkyl	5.28
		PHE409	Pi-alkyl	5.12
		PRO410	Pi-alkyl	5.06
		LYS518	Alkyl	4.14
		PRO410	Pi-alkyl	5.15
		ASN403	Conventional hydrogen bond	2.73
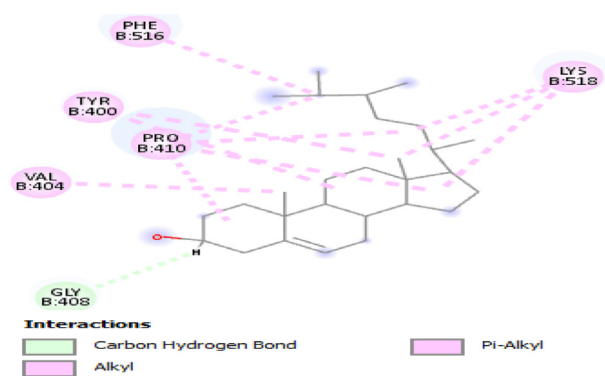
Figure 10: 2D Interaction of campesterol (**1**) with crystal structure of *S. aureus* (PDB: 3HO8).

and ciprofloxacin, thus indicating their importance in *P. aeruginosa* inhibition. The pathogen is a multidrug-resistant bacterium that causes illness in both plants and animals, such as septic shock, pneumonia, gastro-intestinal conditions, and urinary tract infection.[29] β-sitosterol has also been discovered in *Fiscus religiosa*, and has been found to substantially interact with binding sites of the Kelch-Neh2 complex (PDB: 2FLU) crystal structure, thus suggesting that it is a potential competitive drug to counteract Keapl and may be applied in cancer chemoprevention.[28]
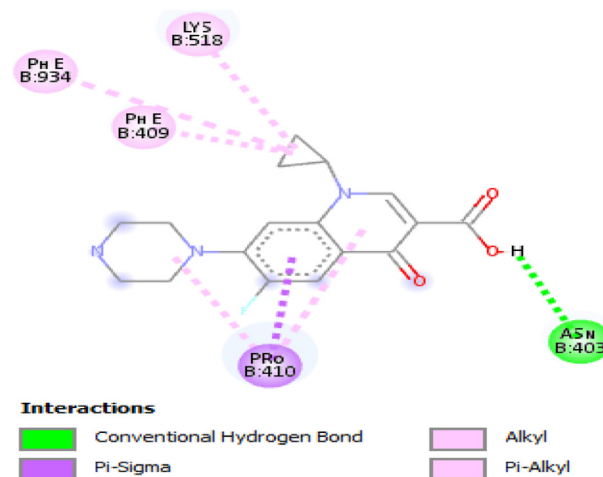

Figure 11: 2D Interaction of β-sitosterol (**2**) with crystal structure of *S. aureus* (PDB: 3HO8).
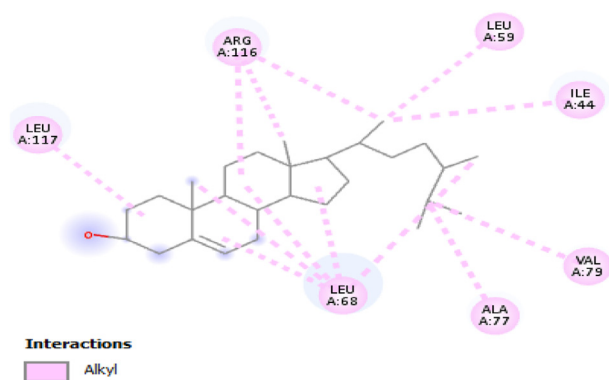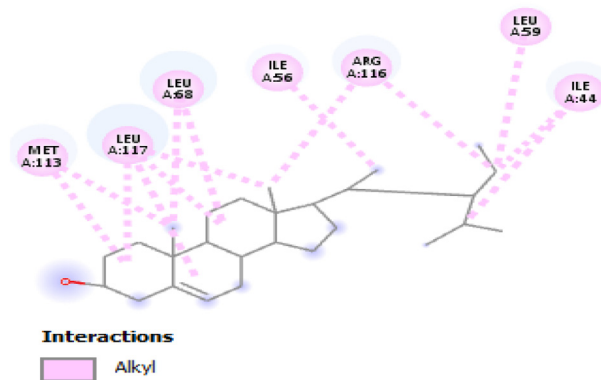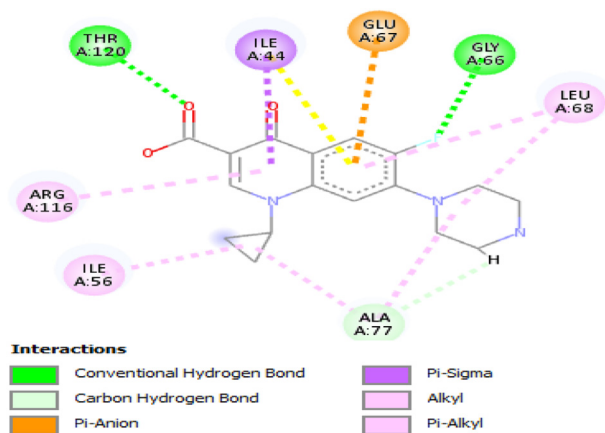

Figure 12: 2D Interaction of ciprofloxacin with crystal structure of *S. aureus* (PDB: 3HO8).

Table 4: Results of binding energy of isolated compounds/ciprofloxacin with receptor (PDB: 2OZ6).

Ligands	Binding score (kcal/mol)	Protein interaction	Types of interaction	Bond distance Å
Campesterol	−7.9	ALA77	Alkyl	3.79
		LEU59	Alkyl	4.43
		ILE44	Alkyl	4.22
		VAL79	Alkyl	5.46
		ARG116	Alkyl	5.26
		ARG116	Alkyl	4.05
		ARG116	Alkyl	5.57
		LEU117	Alkyl	4.92
		LEU68	Alkyl	3.82
		LEU68	Alkyl	5.42
		LEU68	Alkyl	4.48
		LEU68	Alkyl	4.48
		LEU68	Alkyl	4.42
β-sitosterol	−7.7	ILE56	Alkyl	4.16
		ILE44	Alkyl	4.44
		ILE44	Alkyl	3.95
		LEU59	Alkyl	4.25
		ARG116	Alkyl	4.20
		ARG116	Alkyl	4.50
		LEU68	Alkyl	4.70
		LEU68	Alkyl	4.84
		MET113	Alkyl	4.74
		MET113	Alkyl	4.32
		LEU117	Alkyl	4.16
		LEU117	Alkyl	5.03
		LEU117	Alkyl	4.25
		LEU117	Alkyl	4.19
Ciprofloxacin	−8.7	GLU57	Pi-anion	4.48
		ILE44	Pi-sigma	3.99
		ALA77	Carbon hydrogen bond	2.52
		LEU68	Alkyl	4.76
		ALA77	Alkyl	5.14
		ALA77	Alkyl	4.72
		ILE56	Alkyl	4.42
		ALA77	Alkyl	4.72
		ARG116	Pi-alkyl	4.84
		LEU68	Pi-alkyl	5.43
		ILE44	Pi-alkyl	4.16
		THR120	Conventional hydrogen bond	2.37
		GLY66		2.37

Figure 13: 2D Interaction of campesterol (**1**) with crystal structure of *P. aeruginosa* (PDB: 2OZ6).

Figure 14: 2D Interaction of β-sitosterol (**2**) with crystal structure of *P. aeruginosa* (PDB: 2OZ6).

Figure 15: 2D Interaction of ciprofloxacin with crystal structure of *P. aeruginosa* (PDB: 2OZ6).

Conclusion

The structures of two compounds (campesterol and β-sitosterol) isolated from *S. innocua* root bark were characterized with MS and NMR spectroscopy. In the docking study, campesterol and β-sitosterol showed binding energies of −7.8 and −7.7 kcal/mol with the binding site of *S. aureus* (PDB: 3HO8), values higher than that of ciprofloxacin. Furthermore, the compounds showed binding energies of −7.9 and 7.7 kcal/mol with the *P. aeruginosa* binding site (PDB: 2OZ6), values slightly lower than that of ciprofloxacin (−8.7 kcal/mol). These findings suggest that the compounds might serve as potential antibacterial agents.

Source of funding

Conflict of interest

The authors have declared no competing interests.

Ethical approval

Not applicable.

Authors contributions

MSS developed the procedure for isolation, AJU performed the experiments/wrote the manuscript, ORI assisted in supervising the experiment, and HI contributed to NMR elucidation. All authors have critically reviewed and approved the final draft and are responsible for the content and similarity index of the manuscript.

Acknowledgment

References

1. Sasidharan S, Chen Y, Saravanan D, Sundram KM, Latha LY. Extraction, isolation and characterization of bioactive compounds from plants extracts. **Afr J Tradit Complementary Altern Med 2011**; 8(1): 1−10. PMID: 22238476.

2. Umaru I, Badruddin FA, Umaru HA. Extraction, isolation and characterization of new compound and anti-bacterial potentials of the chemical constituents compound from *Leptadenia hastata* leaf extract. **ChemRxiv 2019**. https://doi.org/10.26434/chemrxiv.9782585.v2.

3. Mondal M, Hossain MS, Das N, Khalipha ABR, Sarkar AP, Islam MT, et al. Phytochemical screening and evaluation of pharmacological activity of leaf methanol extract of *Colocasia affinis* Schott. **Clin Phytosci. 2019**; 5(8): 1−11. https://doi.org/10.1186/s40816-019-0100-8.

4. Uttu AJ, Sallau MS, Iyun ORA, Ibrahim H. Recent advances in isolation and antimicrobial efficacy of selected *Strychnos* species: a mini review. **J Chem Rev 2022**; 4(1): 15−24. https://doi.org/10.22034/JCR.2022.314381.1129.

5. Choi J, Lee E, Lee H, Kim K, Ahn K, Shim B, et al. Identification of campesterol from *Chrysanthemum coronarium* L. and its antiantiogenic activities. **Phytother Res 2007**; 21(10): 954−959. https://doi.org/10.1002/ptr.2189.

6. Jian P, Sharma HP, Basri F, Baraik B, Kumari S, Pathak C. Pharmacological profiles of ethno-medicinal plant: *Plumbago zeylanica* I. − a review. **Int J Pharmaceut Sci Rev Res 2014**; 24(1): 157−163.

7. Nour EA, Abd E, Khaled E, Maher AE, Samir AS, Mostafa ME. Designed, synthesis, molecular docking and *in silico* ADMET profile of pyrano[2,3-d]pyrimidine derivatives as antimicrobial and anticancer agents. **Bioorg Chem 2021**; 115: 1051186. https://doi.org/10.1016/j.bioorg.2021.105186.

8. Emmanuel IE, Uttu AJ, Oluwaseye A, Hassan S, Ajala A. A semi-empirical based QSAR study of indole β-diketo acid, diketo acid and carboxamide derivatives as potent HIV-1 agent using quantum chemical descriptors. **IOSR J Appl Chem 2015**; 8(11i): 12−20. https://doi.org/10.9790/5736-081111220.

9. Ruffo CK, Birnie A, Tengnas B. *Edible wild plants of Tanzania.* Nairobi: Regional Land Management Unit; 2002.

10. Orwa CA, Mutua KR, Jamnadass R, Anthony S. *Agroforestree database: a tree reference and selection guide version 4.0*; 2009. Retrieved from, http://www.worldagroforestry.org/sites/treedbs/treedatabases.asp.

11. Ibrahim H, Uttu AJ, Sallau MS, Iyun ORA. Gas chromatography−mass spectrometry (GC−MS) analysis of ethyl acetate root bark extract of S*trychnos innocua* (Delile). **Beni-Suef Univ J Basic Appl Sci 2021**; 10: 1−8. https://doi.org/10.1186/s43088-021-00156-1. 65.

12. Iyun ORA, Uttu AJ, Sallau MS, Ibrahim H. GC-MS analysis of methanol extract of *Strychnos innocua* (Delile) root bark. **Adv J Chem A 2022**; 5(2): 104−117. https://doi.org/10.22034/AJCA.2022.322806.1295.

13. Sallau MS, Uttu AJ, Iyun ORA, Ibrahim H. *Strychnos innocua* (Delile): phytochemical and antimicrobial evaluations of its root bark extracts. **Adv J Chem B 2022**; 4(2022): 17−28. https://doi.org/10.22034/ajcb.2022.323148.1104.

14. Uttu AJ, Sallau MS, Iyun ORA, Ibrahim H. Coumarin and fatty alcohol from root bark of *Strychnos innocua* (Delile): isolation, characterization and in silico molecular docking studies. **Bull Natl Res Cent 2022**; 46(174): 1−12. https://doi.org/10.1186/s42269-022-00862-5.

15. Uttu AJ, Sallau MS, Iyun ORA, Ibrahim H. Isolation, characterization and in silico molecular docking studies of two terpenoids from *Strychnos innocua* (Delile) root bark for antibacterial properties. **Adv J Chem A 2022**; 5(3): 241−252. https://doi.org/10.22034/AJCA.2022.344451.1315.

16. Ejeh S, Uzairu A, Shallangwa GA, Abechi SE. Computational techniques in designing a series of 1,3,4-trisubstituted pyrazoles as unique hepatitis C virus entry inhibitors. **Chem Rev Lett 2021**; 4: 108−119. ISSN: 2645-4947.

17. Tukur A, Habila JD, Ayo RG, Iyun ORA. Design, synthesis, docking studies and antibiotic evaluation (in vitro) of some novel (*E*)-4-(3-(diphenylamino)phenyl)- 1-(4-methoxyphenyl)-2-methylbut-3-en-1-one and their analogues. **Bull Natl Res Cent 2022**; 46(60): 1−12. https://doi.org/10.1186/s42269-022-00745-9.

18. Musa WJ, Duengo S, Kilo AK. Campesterol from methanol fraction of *Brotowali* (*Tinospora crispa*) stem bark. **Atlantis Highlights Chem Pharmaceut Sci 2019**; 1: 95−97.

19. Pham XP, Nhung TTT, Trinh HN, Trung DM, Giang DT, Vu BD, et al. Isolation and structural characterization of compounds from *Blumea lacera*. **Pharmacogn J 2021**; 13(4): 999−1004. https://doi.org/10.5530/pj.2021.13.129.

20. Aliba MO, Ndukwe IG, Ibrahim H. Isolation and characterization of β-sitosterol from methanol extracts of the stem bark of large leaved rock fig (*Ficus aburilifolia* Mig). **J Appl Sci Environ Manag 2018**; 22(10): 1639−1642.

21. Erwin U, Pusparohmana WR, Safitry RD, Marliana E, Usman E, Kusuma IW. Isolation and characterization of stigmasterol and β-sitosterol from wood bark extract of *Baccaurea macrocarpa* Miq. Mull. Arg. **Rasayan J Chem 2020**; 13(4): 2552−2558. https://doi.org/10.31788/RJC.2020.1345652.

22. Jain PS, Bari SB. Isolation of lupeol, stigmasterol and campesterol from petroleum ether extract of woody stem of *Wrightia tinctoria*. **Asian J Plant Sci 2010**; 9(3): 163−167. ISSN: 1682-3974.

23. Okoro IS, Tor-Anyiin TA, Igoli JO, Noundou XS, Krause RWM. Isolation and characterisation of stigmasterol and β−sitosterol from *Anthocleista djalonensis* A. Chev. **Asian J Chem Sci 2017**; 3(4): 1−5. ISSN: 2456-7795.

24. Choi NH, Jang JY, Choi GJ, Choi YH, Jang KS, Nguyen VT, et al. Antifungal activity of sterols and dipsacus saponins isolated from *Dipsacus asper* roots against phytopathogenic fungi. **Pestic Biochem Physiol 2017**; 141: 103−108. https://doi.org/10.1016/j.pestbp.2016.12.006.

25. Singh B, Singh JP, Shevkani K, Singh N, Kaur A. Bioactive constituents in pulses and their health benefits. **J Food Sci Technol 2017**; 54(4): 858−870. https://doi.org/10.1007/s13197-016-2391-9.

26. Moreau RA, Nystrom L, Whitaker BD, Winkler-Moser JK, Baer DJ, Gebauer SK, et al. Phytosterols and their derivatives: structural diversity. Distribution, metabolism, analysis, and health-promoting uses. **Prog Lipid Res 2018**; 70: 35−61. https://doi.org/10.1016/j.plipres.2018.04.001.

27. Dalen RV, Peschel A, Sorge NM. Wall teichoic acid in *Staphylococcus aureus* host interaction. **Trends Microbiol 2020**; 28(12): 985−998. https://doi.org/10.1016/j.tim.2020.05.017.

28. Syahputra HD, Masfria M, Hasibuan PAZ, Iksen I. In silico docking studies of phytosterol compounds selected from *Ficus religiosa* as potential chemopreventive agent. **Rasayan J Chem 2022**; 15(2): 1080−1084. https://doi.org/10.31788/RJC.2022.1526801.

29. Diggle S, Whiteley M. Microbe profile: *Pseudomonas aeruginosa*: opportunistic pathogen and lab rat. **Microbiology 2020**; 166(1): 30−33. https://doi.org/10.1099/mic.0.000860.